

Technical Notes

TECHNICAL NOTES are short manuscripts describing new developments or important results of a preliminary nature. These Notes should not exceed 2500 words (where a figure or table counts as 200 words). Following informal review by the Editors, they may be published within a few months of the date of receipt. Style requirements are the same as for regular contributions (see inside back cover).

Aeroelastic Tailoring of Composite Wing Structures by Laminate Layup Optimization

Shijun Guo*

Cranfield University, Cranfield, Bedford, MK43 0AL
England, United Kingdom

and

Wenyuan Cheng† and Degang Cui‡

Beijing University of Aeronautics and Astronautics, Beijing,
People's Republic of China

DOI: 10.2514/1.20166

Introduction

PREVIOUS research showed that elastic coupling and warping restraint might have a positive effect on aeroelastic stability of forward-swept composite wings [1–4]. The work encouraged subsequent investigation into the optimization of composite wing structures for desirable aeroelastic behavior [5–8]. The research has demonstrated that a significant increase of flutter speed can be achieved by optimizing the wing skin thickness or the laminate layups considering the effect of bending–torsion coupling [7,8]. However, the impact of wing geometry upon the influence of stiffness coupling on the aeroelastic optimization has received little attention. This current research is therefore aimed at investigating the effect of swept angle, taper ratio, and mass distribution on aeroelastic tailoring of a composite wing. Six aeroelastic tailoring cases of a composite wing by optimizing the wing box laminate layups have been considered. A classical gradient-based deterministic *GD* optimization method and a genetic algorithm *GA* have been employed for comparison purposes. It was noted that the optimized layup solution by using the *GD* method largely depends on the setting of initial design variables. Nevertheless, this method is efficient and normally produces an optimal result at each step of the optimization process before converging to the final optimal solution. Comparing with the *GD* method, the *GA* approach is more robust and produces optimal solutions with little influence from the initial layup despite the need for much more computational time. The example considered in this paper has shown that optimized layups resulting in a maximum increase of flutter speed can be achieved by employing either the *GD* or *GA* method. However, wing geometry

and mass distribution have significant influence on aeroelastic tailoring results.

Methodology

In this paper, a generic example of high aspect ratio composite wing as illustrated in Fig. 1 has been analyzed. The wing primary structure was modeled by an assembly of single-cell thin-walled box beams enclosed between the spars. Leading and trailing edge cells contributed to mass and inertia, and were counted for aerodynamic force calculation only. Based on the geometry, properties, and laminate layups, the bending, torsion, and bending–torsion coupling rigidities for each of the box beams were obtained using the method developed in [9–11]. Using the dynamic stiffness matrix (DSM) method [12,13] and neglecting the shear deformation and warping effect, the governing equations for a box beam in free vibration are represented below:

$$EI \frac{\partial^4 h}{\partial y^4} + CK \frac{\partial^3 \phi}{\partial y^3} + m \frac{\partial^2 h}{\partial t^2} - m X_\alpha \frac{\partial^2 \phi}{\partial t^2} = 0 \quad (1)$$

$$GJ \frac{\partial^2 \phi}{\partial y^2} + CK \frac{\partial^3 h}{\partial y^3} + m X_\alpha \frac{\partial^2 h}{\partial t^2} - I_p \frac{\partial^2 \phi}{\partial t^2} = 0 \quad (2)$$

where EI , GJ , and CK are bending, torsion, and bending–torsion coupling rigidities, m and I_p are, respectively, the mass and polar mass moment of inertia per unit length of the wing box beam, X_α is the distance between the mass and geometric elastic axes, and h and ϕ represent the transverse and rotational displacements of the wing box beam as illustrated in Fig. 2a.

By solving the above differential equations, an exact solution for displacements at both ends of the beam can be obtained and related to the associated forces. This resulted in a DSM for each of the beams, which was assembled along the wingspan to form the DSM for the whole wing box structure. The nonstandard eigenvalue problem produced by the frequency dependent DSM was solved by using the Wittrick and William algorithm [14].

By using the normal mode method, the flutter equation for an oscillating wing can be written in generalized coordinates as

$$\{[K_D(\omega)] - \frac{1}{2}\rho V^2[Q A]_R + i\omega[D] + i\frac{1}{2}\rho V^2[Q A]_I\}\{q\} = 0 \quad (3)$$

where ω represents the circular frequency of the wing structure, ρ and V the air density and air velocity, $[K_D(\omega)]$ and $[D]$ the generalized dynamic stiffness and damping matrix of the structure in generalized coordinate $\{q\}$, $[Q A]_R$ and $[Q A]_I$ the real and imaginary parts of the generalized unsteady aerodynamic forces in matrix, which are calculated by using the lifting surface theory [15] in incompressible airflow. The flutter speed and frequency were then calculated by searching and matching the results with the input frequency and speed in subsonic speed range using the *V-g* method.

In the unconstrained optimization represented below, effort was primarily focused on achieving a maximum flutter speed by tailoring the wing box skin and spar web laminate fiber orientations without constraining the structural strength and altering the weight.

Presented as Paper 2132 at the AIAA/ASME/ASCE/AHS/ASC 46th Structures, Structural Dynamics, and Materials Conference; AIAA/ASME/AHS 13th Adaptive Structures Conference, Austin, TX, 18–21 April 2005; received 21 September 2005; accepted for publication 4 October 2006. Copyright © 2006 by the American Institute of Aeronautics and Astronautics, Inc. All rights reserved. Copies of this paper may be made for personal or internal use, on condition that the copier pay the \$10.00 per-copy fee to the Copyright Clearance Center, Inc., 222 Rosewood Drive, Danvers, MA 01923; include the code \$10.00 in correspondence with the CCC.

*Senior Lecturer, Department of Aerospace Engineering, School of Engineering, Member AIAA.

†Research Student, Department of Aeronautical Science and Engineering.

‡Professor, Department of Aeronautical Science and Engineering.

$$\text{Minimize } f_v(\alpha) = \left[1 - \frac{V_f(\alpha) - V_f(\alpha_0)}{V_f(\alpha_0)} \right]^2 \quad (4)$$

within $-90 \leq \{\alpha\} \leq 90$

where $\{\alpha_0\}$ and $\{\alpha\}$ represent a set of fiber orientations for a laminate as design variables specified by the user in the beginning of optimization and optimized during the process, respectively, $V_f(\alpha)$ is a resulting flutter speed of the wing corresponding to $\{\alpha\}$, and $f_v(\alpha)$ is an objective function. A gradient-based deterministic (GD) method [16,17] has been employed for solving the optimization problem.

The generic algorithm GA has been used as an alternative optimization method based on the numerical simulation of natural selection and evolution in Darwin's theory. The GA process was started with an initial randomized population with each of the design variables α_i being represented by a binary unsigned integer β_i of length l_i called substring. For each selected β and resulting flutter speed, a value of the fitness function $F(\beta) = V_f(\alpha)$ was calculated. The GA evolved using three operators for the next generation reproduction. First, a mating pool was selected based on the probability of $F(\beta)$ in a proportional selection method. This was followed by a selection of mates, a double-spot crossover proceeds by random selection of crossing sites of the mated string couples based on an adaptive probability of crossover. Finally, mutation was performed for each string on a bit-by-bit basis. Consequently, a set of optimized variables was selected as a new generation and the fitness values were evaluated. The above procedure was performed in an iterative manner until a convergence condition was satisfied.

Examples of Aeroelastic Optimization

In structural modeling of the wing example as illustrated in Fig. 1, the wing box was divided into five spanwise box beams. Each of them was divided into four panels along the circumference representing the skins and spar webs as shown in Fig. 2b. This results in the whole wing box being modeled by 20 laminated panels. In each of the 16-layer carbon fiber epoxy laminated panels, two neighboring plies of thickness 0.5 mm were grouped as one design variable to keep their fiber orientations consistent during the optimization. For the whole wing box, the total number of independent design variables was 160 or 80 in a symmetric layup case. The composite material properties are $E_1 = 140$ GPa, $E_2 = 9.5$ GPa,

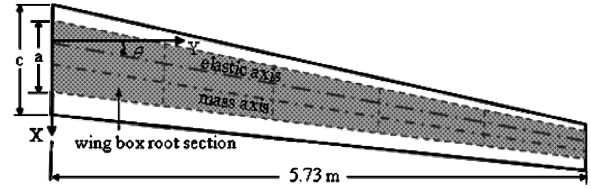


Fig. 1 General layout and dimension of the swept-back composite wing.

$G_{12} = 5.8$ GPa, and density $\rho = 1562$ Kg/m³. Six design study cases with different wing swept angle, taper ratio, and mass are considered. The $[(\pm 45)_4]_s$ layup associated with the maximum torsional rigidity GJ was chosen as a benchmark in each case to compare with the optimized solutions.

First, the GD method was employed in conducting the aeroelastic tailoring. The results are presented in Table 1. In case 1, a nonswept uniform wing box with dimensions $a = 0.80$, $b = 0.37$, $c = 1.22$, $d_1 = 0.07$, $d_2 = 0.05$ m as shown in Fig. 2b was considered. Comparing with the benchmark case 1.1, the results in case 1.2 show that the flutter speed V_f has been increased by 5.1% by keeping the laminate layups in all the box beams uniform during the optimization. When the laminate layups in each of the spanwise box beams were tailored independently in case 1.3, a significantly greater increase of V_f , up to 20%, has been achieved. The results in both cases 1.2 and 1.3 indicate that the bending–torsional coupling rigidity CK has played a beneficial role in the aeroelastic tailoring.

In case 2, the same uniform wing is swept back at $\theta = 20$ deg. Although the swept angle leads to a 3.5% increase of V_f in the layup case 2.1 compared with the nonswept case 1.1, the effect of CK on V_f appears to be less significant. As shown in Table 1, only a 2.5 and 5.8% increase of V_f has been achieved in cases 2.2 and 2.3, respectively, against case 2.1.

In cases 3 and 4, the wing box is geometrically tapered at a ratio of 0.57 with dimensions $a = 0.97$, $b = 0.55$, $c = 1.45$, $d_1 = 0.105$, $d_2 = 0.075$ m as shown in Fig. 2b. However, the spanwise mass and inertia distribution were artificially kept uniform. As shown in Table 2, an increase of V_f by 2.3 and 6.1% has been obtained in the nonswept wing cases 3.2 and 3.3, respectively, comparing with case 3.1. When the wing was swept back at $\theta = 20$ deg, a further increase of V_f up to 8 and 9.4% has been achieved in cases 4.2 and

Table 1 Optimized results for a uniform wing box, cases 1 and 2

Cases 1 and 2	Layup in top and bottom skins, front and rear spar webs, degree	Bending, torsion, and coupling rigidity, MN · m ²	Flutter speed, m/s, and frequency, rad/s
1.1 maximum GJ layup	$[45/-45/45/-45]_s$ for all skin and spar web laminates	EI = 0.1217 GJ = 0.7766 CK = 0.00	$V_f = 176.0$ $\omega_f = 101.8$
1.2 uniform-section optimization	$[50.4/-45.0/46.5/-45.0]_s$ $[-45.1/46.3/-45.2/46.2]_s$ $[-44.9/44.8/-45.2/44.8]_s$ $[47.2/-43.3/46.8/-43.6]_s$	EI = 0.1160 GJ = 0.7727 CK = -0.0092	$V_f = 185.0$ (up by 5.1%) $\omega_f = 85.7$
1.3 ^a multisection optimization	$[79.4/-29.0/90.0/-36.6]_s$ $[-71.5/43.5/-71.8/19.4]_s$ $[-48.9/41.1/-48.9/37.6]_s$ $[41.9/-51.6/37.4/-47.3]_s$	EI = 0.2393 GJ = 0.4408 CK = -0.1987	$V_f = 211.0$ (up by 20%) $\omega_f = 43.3$
2.1 maximum GJ layup	$[45/-45/45/-45]_s$ for all skin and spar web laminate	EI = 0.1217 GJ = 0.7766 CK = 0.00	$V_f = 182.2$ $\omega_f = 94.8$
2.2 uniform-section optimization	$[33.5/-44.3/33.5/-44.3]_s$ $[-35.6/39.8/-35.6/39.8]_s$ $[-30.0/30.0/-30.0/30.0]_s$ $[30.0/-30.0/30.0/-30.0]_s$	EI = 0.1934 GJ = 0.7058 CK = 0.070	$V_f = 186.7$ (up by 2.5%) $\omega_f = 76.8$
2.3 ^a multisection optimization	$[49.0/-35.0/74.0/-35.0]_s$ $[-60.0/43.0/-66.0/43.0]_s$ $[-30.0/30.0/-30.0/30.0]_s$ $[30.0/-30.0/30.0/-30.0]_s$	EI = 0.1667 GJ = 0.6260 CK = -0.1518	$V_f = 192.7$ (up by 5.8%) $\omega_f = 69.2$

^aThe layups and rigidities shown are at root section only.

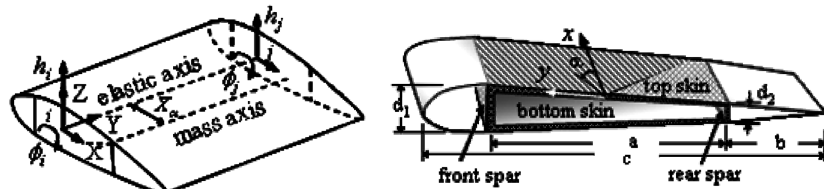


Fig. 2 a) The displacements and b) cross section details of a wing box beam element.

4.3, respectively. The results indicate that the role of *CK* in aeroelastic tailoring remains at least as effective as the uniform wing box.

In case 5 where the wing box was tapered in geometry, mass, and inertia, the potential beneficial effect of *CK* on V_f appeared to be

largely reduced. As presented in Table 3, only a 0.2 and 1.8% increase of V_f has been achieved in cases 5.2 and 5.3, respectively, by uniform and multisection optimization. When the tapered wing was swept back at $\beta = 20^\circ$ in case 6, only slightly better results were obtained in cases 6.2 and 6.3, as shown in Table 3.

Table 2 Optimized results for a tapered wing of uniform mass, cases 3 and 4

Cases 3 and 4	Layup in top and bottom skins, front and rear spar webs, degree	Bending, torsion, and coupling rigidity, $\text{MN} \cdot \text{m}^2$	Flutter speed, m/s, and frequency, rad/s
3.1 maximum <i>GJ</i> layup	$[45/-45/45/-45]_s$ for all skin and spar web laminates	$EI = 0.2167$ $GJ = 1.3825$ $CK = 0.0$	$V_f = \mathbf{202.6}$ $\omega_f = 123.0$
3.2 uniform-section optimization	$[44.1/-45.7/46.6/-45.0]_s$ $[43.6/-46.6/43.6/-45.0]_s$ $[44.8/-45.4/44.6/-45.0]_s$ $[44.8/-45.4/44.6/-45.0]_s$	$EI = 0.2181$ $GJ = 1.3800$ $CK = -0.0217$	$V_f = \mathbf{207.3}$ (up by 2.3%) $\omega_f = 105.1$
3.3 ^a multisection optimization	$[44.5/-46.0/45.9/-44.1]_s$ $[44.6/-45.4/33.9/-51.0]_s$ $[45.0/-45.3/44.5/-45.1]_s$ $[39.3/-50.6/43.1/-45.0]_s$	$EI = 0.2450$ $GJ = 1.3450$ $CK = -0.0811$	$V_f = \mathbf{214.9}$ (up by 6.1%) $\omega_f = 96.3$
4.1 maximum <i>GJ</i> layup	$[45/-45/45/-45]_s$ for all skin and spar web laminate	$EI = 0.2167$ $GJ = 1.3825$ $CK = 0.0$	$V_f = \mathbf{215.0}$ $\omega_f = 101.5$
4.2 uniform-section optimization	$[45.0/-45.3/45.0/-45.3]_s$ $[47.0/-45.1/50.7/-39.8]_s$ $[45.0/-45.0/46.6/-44.9]_s$ $[44.1/-45.8/45.1/-40.4]_s$	$EI = 0.2195$ $GJ = 1.3680$ $CK = 0.0621$	$V_f = \mathbf{232.2}$ (up by 8%) $\omega_f = 81.2$
4.3 ^a multisection optimization	$[45.2/-44.8/49.7/-44.8]_s$ $[45.1/-45.2/45.0/-45.0]_s$ $[45.0/-45.0/45.1/-45.0]_s$ $[45.0/-44.2/45.0/-45.0]_s$	$EI = 0.2132$ $GJ = 1.3780$ $CK = -0.0214$	$V_f = \mathbf{235.3}$ (up by 9.4%) $\omega_f = 80.8$

^aThe layups and rigidities shown are at root section only.

Table 3 Optimized results for a tapered wing, cases 5 and 6

Cases 5 and 6	Layup in top and bottom skins, front and rear spar webs, degree	Bending, torsion, and coupling rigidity, $\text{MN} \cdot \text{m}^2$	Flutter speed, m/s, and frequency, rad/s
5.1 maximum <i>GJ</i> layup	$[45/-45/45/-45]_s$ for all skin and spar web laminates	$EI = 0.2167$ $GJ = 1.3825$ $CK = 0.0$	$V_f = \mathbf{202.6}$ $\omega_f = 123.0$
5.2 uniform-section optimization	$[45.2/-45.0/45.0/-45.1]_s$ $[-45.0/45.0/-45.0/45.0]_s$ $[-49.5/44.4/-45.6/44.5]_s$ $[45.0/-45.0/45.0/-45.0]_s$	$EI = 0.2125$ $GJ = 1.378$ $CK = -0.020$	$V_f = \mathbf{203.0}$ (up by 0.2%) $\omega_f = 123.4$
5.3 ^a multisection optimization	$[45.5/-44.5/45.4/-44.6]_s$ $[-44.6/45.4/-44.6/45.4]_s$ $[-44.6/44.7/-45.3/44.9]_s$ $[45.5/-44.6/45.4/-44.5]_s$	$EI = 0.2166$ $GJ = 1.382$ $CK = 0.001$	$V_f = \mathbf{206.3}$ (up by 1.8%) $\omega_f = 117.0$
6.1 maximum <i>GJ</i> layup	$[45/-45/45/-45]_s$ for all skin and spar web laminate	$EI = 0.2167$ $GJ = 1.3825$ $CK = 0.0$	$V_f = \mathbf{207.2}$ $\omega_f = 116.2$
6.2 uniform-section optimization	$[43.6/-56.2/44.9/-51.5]_s$ $[-45.1/46.3/-45.1/46.3]_s$ $[-45.0/45.0/-45.0/45.0]_s$ $[45.0/-45.0/45.0/-45.0]_s$	$EI = 0.2048$ $GJ = 1.3492$ $CK = 0.0814$	$V_f = \mathbf{208.5}$ (up by 0.6%) $\omega_f = 112.5$
6.3 ^a multisection optimization	$[44.9/-45.1/45.1/-44.9]_s$ $[-45.1/44.9/-45.1/44.8]_s$ $[-45.0/45.0/-45.0/45.0]_s$ $[45.0/-45.0/45.0/-45.0]_s$	$EI = 0.2168$ $GJ = 1.382$ $CK = -0.0021$	$V_f = \mathbf{215.2}$ (up by 3.9%) $\omega_f = 104.2$

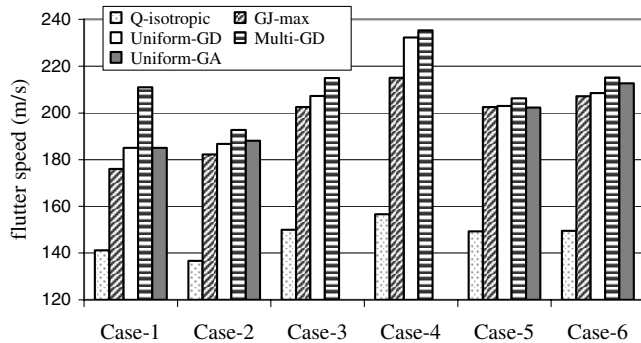
^aThe layups and rigidities shown are at root section only.

Table 4 Optimization results by GA method

Optimized results	Case 1.2	Case 2.2	Case 5.2	Case 6.2
Layup in top skin	$[(45.1/-52.1)_2]_s$	$[(-39.4/39.2)_2]_s$	$[(45.0/-47.0)_2]_s$	$[(44.3/-50.8)_2]_s$
Bottom skin	$[(-44.8/47.3)_2]_s$	$[(-35.1/52.2)_2]_s$	$[(-55.0/49.0)_2]_s$	$[(63.9/-40.0)_2]_s$
Front spar web	$[(-53.3/54.6)_2]_s$	$[(-42.6/43.0)_2]_s$	$[(43.0/-46.0)_2]_s$	$[(-47.7/41.0)_2]_s$
Rear spar web	$[(35.9/-37.7)_2]_s$	$[(-44.1/25.3)_2]_s$	$[(-37.0/43.0)_2]_s$	$[(-41.1/23.9)_2]_s$
Rigidity, $MN \cdot m^2$, in bending	$EI = 0.11309$	$EI = 0.16267$	$EI = 0.2169$	$EI = 0.22900$
Torsion	$GJ = 0.76002$	$GJ = 0.71043$	$GJ = 1.3730$	$GJ = 1.22050$
Coupling	$CK = 0.04206$	$CK = 0.08606$	$CK = -0.1341$	$CK = 0.22283$
Flutter speed, m/s	$V_f = 185.0$	$V_f = 188.0$	$V_f = 202.3$	$V_f = 212.7$
Frequency, rad/s	$\omega_f = 102.5$	$\omega_f = 70.0$	$\omega_f = 122.9$	$\omega_f = 81.6$

References

- [1] Librescu, L., and Khdeir, A. A., "Aeroelastic Divergence of Swept-Forward Composite Wings Including Warping Restraint Effect," *AIAA Journal*, Vol. 26, No. 11, Nov. 1988, pp. 1373–1377.
- [2] Librescu, L., and Simovich, J., "General Formulation for the Aeroelastic Divergence of Composite Swept-Forward Wing Structures," *Journal of Aircraft*, Vol. 25, No. 4, 1988, pp. 364–371.
- [3] Librescu, L., and Thangjitham, S., "Analytical Study on Static Aeroelastic Behavior of Swept-Forward Composite Wing Structures," *Journal of Aircraft*, Vol. 28, No. 2, 1991, pp. 151–157.
- [4] Lottati, I., "Flutter and Divergence Aeroelastic Characteristics for Composite Forward Swept Cantilever Wing," *Journal of Aircraft*, Vol. 22, No. 11, Nov. 1985, pp. 1001–1007.
- [5] Guo, S., Cheung, C. W., Banerjee, J. R., and Butler, R., "Gust Alleviation and Flutter Suppression of an Optimised Composite Wing," *Proceedings of the International Forum on Aeroelasticity and Structural Dynamics*, Royal Aeronautical Society, London, 1995, pp. 41.1–41.9.
- [6] Georgiades, G. A., Guo, S., and Banerjee, J. R., "Flutter Characteristics of Laminated Wings," *Journal of Aircraft*, Vol. 33, No. 6, 1996, pp. 1204–1206.
- [7] Lillico, M., Butler, R., Guo, S., and Banerjee, J. R., "Aeroelastic Optimisation of Composite Wings Using the Dynamic Stiffness Method," *The Aeronautical Journal*, Vol. 101, No. 1002, Feb 1997, pp. 77–86.
- [8] Guo, S., Banerjee, J. R., and Cheung, C. W., "The Effect of Laminate Layup on the Flutter Speed of Composite Wings," *Proceedings of the Institution of Mechanical Engineers, Part G (Journal of Aerospace Engineering)*, Vol. 217, No. G3, 2003, pp. 115–122.
- [9] Hodges, D. H., Atilgan, A. R., Fulton, M. V., and Rehfield, L. W., "Free Vibration Analysis of Composite Beams," *Journal of the American Helicopter Society*, Vol. 36, No. 3, July 1991, pp. 36–47.
- [10] Berdichevsky, V., Armanios, E. A., and Badir, A. M., "Theory of Anisotropic Thin-Walled Closed Cross-Section Beams," *Composites Engineering*, Vol. 2, No. 5–7, 1992, pp. 411–432.
- [11] Armanios, E. A., and Badir, A. M., "Free Vibration Analysis of Anisotropic Thin-Walled Closed-Cross-Section Beams," *AIAA Paper No. 94-1327-CP*, July 1994, pp. 164–171.
- [12] Banerjee, J. R., and Williams, F. W., "Coupled Bending–torsional Dynamic Stiffness Matrix for Timoshenko Beam Elements," *Computers and Structures*, Vol. 42, No. 3, 1992, pp. 301–310.
- [13] Banerjee, J. R., and Williams, F. W., "Free Vibration of Composite Beams: An Exact Method Using Symbolic Computation," *Journal of Aircraft*, Vol. 32, No. 3, 1995, pp. 636–642.
- [14] Wittrick, W. H., and Williams, F. W., "A General Algorithm for Computing Natural Frequencies of Elastic Structures," *Quarterly Journal of Mechanics and Applied Mathematics*, Vol. 24, No. 3, 1971, pp. 263–284.
- [15] Davies, D. E., "Theoretical Determination of Subsonic Oscillatory Airforce Coefficients," *Aeronautical Research Council Reports and Memoranda 3804*, May 1976.
- [16] Fletcher, R., and Powell, M. J. D., "A Rapidly Convergent Method for Minimisation," *Computer Journal*, Vol. 6, No. 2, 1963, pp. 163–168.
- [17] Fox, R. L., *Optimisation Methods for Engineering Design*, Addison-Wesley, Reading, MA, 1971.

**Fig. 3 Comparison of optimized results by the GD and GA method.**

The GA method was also employed in some of the above cases. Unlike the GD method, the initial layup was randomly selected within the boundary of the design variables and a set of near optimal solutions were produced. As shown in Table 4, the best solutions in terms of V_f obtained by using the GA are very close to the optimized results by the GD method. For example, the difference of V_f between the two methods is below 0.7% in cases 1.2 and 2.2, and up to 2% for the tapered wing box in cases 5.2 and 6.2, although the optimized layups from the two methods are clearly different.

A comparison of the maximum flutter speed results obtained in all the cases is also presented in Fig. 3. In this figure, the result for a wing box made of quasi-isotropic layup $[(0/90/\pm 45)_2]_s$ in each of the cases has also been included for comparison.

Conclusions

Comparing with the quasi-isotropic layup, there is a great potential for increasing the flutter speed by optimizing the fiber orientations of composite wing box laminates in all the cases studied in this paper. Comparing with the layup case that offers the maximum torsion rigidity, however, the effect of swept angle, taper ratio, and especially the mass distribution on aeroelastic tailoring is critical. The most effective tailoring is for a uniform nonswept wing box. In this case, a significant increase in flutter speed can be achieved due to a beneficial aeroelastic effect from the bending–torsion coupling rigidity CK . For a swept or geometrically tapered wing, however, the role of CK in the aeroelastic tailoring and hence the potential increase of flutter speed is largely reduced. In the above cases, the GA is preferable to the GD method. For a wing box tapered in geometry and mass, the influence of CK on aeroelastic tailoring becomes negligible. In this case, the torsion rigidity GJ dominates the flutter speed and the ± 45 laminate layup results in a near global optimum solution. Aeroelastic tailoring can be simplified to a process of searching for the maximum GJ instead of flutter speed. This will not only largely save computational time but also simplify design optimization. In such a case, the GD method is preferable to the GA method.